

UCSF

UC San Francisco Previously Published Works

Title

Wide Dispersion and Diversity of Clonally Related Inhibitory Interneurons.

Permalink

<https://escholarship.org/uc/item/2rn208kb>

Journal

Neuron, 87(5)

ISSN

0896-6273

Authors

Harwell, Corey C
Fuentealba, Luis C
Gonzalez-Cerrillo, Adrian
[et al.](#)

Publication Date

2015-09-01

DOI

10.1016/j.neuron.2015.07.030

Peer reviewed



Published in final edited form as:

Neuron. 2015 September 2; 87(5): 999–1007. doi:10.1016/j.neuron.2015.07.030.

Wide Dispersion and Diversity of Clonally Related Inhibitory Interneurons

Corey C. Harwell^{1,*}, Luis C. Fuentealba^{2,5}, Adrian Gonzalez-Cerrillo¹, Phillip R.L. Parker⁴, Caitlyn C. Gertz^{3,5}, Emanuele Mazzola⁶, Miguel Turrero Garcia¹, Arturo Alvarez-Buylla^{2,5}, Constance L. Cepko⁷, and Arnold Kriegstein^{3,5}

¹Department of Neurobiology, Harvard Medical School, Boston, Massachusetts 02115

²Department of Neurological Surgery, University of California San Francisco, San Francisco, CA 94143, USA

³Department of Neurology, University of California San Francisco, San Francisco, CA 94143, USA

⁴Gladstone Institute for Neurological Disease, San Francisco, CA 94158, USA

⁵Eli and Edythe Broad Center of Regeneration Medicine and Stem Cell Research, San Francisco, CA 94143, USA

⁶Department of Biostatistics, Harvard School of Public Health, Boston, Massachusetts 02115, USA

⁷Departments of Genetics and Ophthalmology and Howard Hughes Medical Institute, Harvard Medical School, Boston Massachusetts 02115, USA

Abstract

The mammalian neocortex is composed of two major neuronal cell types with distinct origins: excitatory pyramidal neurons and inhibitory interneurons, generated in dorsal and ventral progenitor zones of the embryonic telencephalon respectively. Thus, inhibitory neurons migrate relatively long distances to reach their destination in the developing forebrain. The role of lineage in the organization and circuitry of interneurons is still not well understood. Utilizing a combination of genetics, retroviral fate mapping and lineage-specific retroviral barcode labeling, we find that clonally related interneurons can be widely dispersed while unrelated interneurons can be closely clustered. These data suggest that migratory mechanisms related to the clustering of interneurons occur largely independent of their clonal origin.

To whom correspondence should be addressed: corey_harwell@hms.harvard.edu.

Publisher's Disclaimer: This is a PDF file of an unedited manuscript that has been accepted for publication. As a service to our customers we are providing this early version of the manuscript. The manuscript will undergo copyediting, typesetting, and review of the resulting proof before it is published in its final citable form. Please note that during the production process errors may be discovered which could affect the content, and all legal disclaimers that apply to the journal pertain.

Author Contributions

C.C.H., L.C.F., A.A.-B. and A.R.K. designed research; C.C.H., L.C.F., A.G.C., P.R.L.P., C.C.G and M.T.G. conducted experiments. C.L.C. developed the EnvA pseudotyped retroviral library and critically reviewed and edited the manuscript. C.C.H. and E.M. analyzed data. C.C.H. and A.R.K. wrote the manuscript.

Introduction

The cerebral cortex is one of the most intricate structures in the mammalian nervous system and is responsible for complex behaviors associated with cognitive function. Nearly all cortical neurons are produced during a limited time window of cortical neurogenesis that occurs during embryonic development (Miller and Gauthier, 2007). In the dorsal telencephalon, radial glia (RG) that line the lateral ventricles and outer radial glia (oRG) that reside in the subventricular zone divide asymmetrically to produce intermediate progenitor cells (IPCs) and neurons (Hansen et al., 2010; Noctor et al., 2001; Noctor et al., 2004; Wang et al., 2011). In rodents, the IPCs divide symmetrically to produce pairs of excitatory neurons (Haubensak et al., 2004; Noctor et al., 2004). Clonally related excitatory neurons migrate along the scaffold of radial glial fibers to form radial arrays across cortical layers (Noctor et al., 2001; Rakic, 1988; Vasistha et al., 2014).

Recent work has implicated clonal relationships among excitatory pyramidal neurons in the formation of stereotypical cortical microcircuitry (Yu et al., 2009). In contrast, inhibitory interneurons are produced in the embryonic ventral telencephalon and follow a complex migratory route, including a phase of prolonged tangential migration, in order to populate the cortex and hippocampus, as well as subpallial structures such as the striatum and amygdala (Anderson et al., 2002; Anderson et al., 2001; Nery et al., 2002; Tricoire et al., 2011; Wonders and Anderson, 2006). Nearly all GABAergic interneurons in the brain arise in the medial ganglionic eminence (MGE) and caudal ganglionic eminence (CGE) (Butt et al., 2005; Nery et al., 2002; Wonders and Anderson, 2006; Xu et al., 2004).

MGE progenitors mostly give rise to two functionally distinct subtypes of interneurons: parvalbumin (PV)-expressing fast spiking interneurons and somatostatin (SOM)-expressing non-fast-spiking interneurons. MGE progenitors are molecularly defined by the expression of the homeodomain transcription factor Nkx2.1, which is required for interneuron migration and specification of mature interneuron identity (Butt et al., 2008; Nobrega-Pereira et al., 2008). The extrinsic signals involved in regulating the migration and positioning of newborn interneurons have been extensively studied (Marin, 2013). However, the roles of intrinsic determinants, such as clonal lineage, and their possible contribution to the distribution of MGE-derived interneurons remains poorly understood. In this study, we seek to determine the relationship between clonal identity and final position of interneurons by utilizing a retroviral barcode library targeted to infect Nkx2.1-expressing progenitor cells. This approach revealed that single progenitor cells can produce cells of both SOM and PV subtypes; that clonally related interneurons can disperse widely throughout different structural and functional regions of the brain; and that cells from unrelated clones can cluster together with a non-random distribution.

Results

To identify the morphological features and proliferative status of cells in the ventral telencephalon, we performed *in utero* intraventricular retrovirus injections in embryonic mouse embryos at gestational day 12.5 (E12.5) (Walantus et al., 2007), coinciding with peak neurogenesis (Butt et al., 2005; Miyoshi et al., 2007). We examined interneuron progenitor

cells in the MGE (Anderson et al., 2001) 24–90 h after infection (Figure 1A–C). MGE progenitors infected with GFP-expressing retroviruses produced radial clusters of cells similar to those previously observed in the dorsal telencephalon (Noctor et al., 2001). Examination of the MGE 24 h after injection revealed either single cells or multi-cell clones primarily composed of two cells, typically both Ki67-positive (Figure 1A). Nearly all Ki67-positive cells at this time point were RG or IPCs based upon known morphological features (97%, n=4 brains, 35 cells) (Noctor et al., 2004). At later time points (48–90 h), clonal clusters consisted of two to eight cells (3.12 ± 1.26 cells per cluster at 48 h, n=49 clusters) containing one RG cell with a single apical process attached to the ventricular surface, along with several presumptive multipolar IPCs and newborn neurons (Figure 1B–C).

To examine the division patterns of these progenitors, we made organotypic slices 24 h after *in utero* intraventricular injection of GFP-expressing retrovirus at E12.5, and monitored cell divisions by time-lapse microscopy. We were able to observe nine divisions of MGE cells with RG morphology, and in each imaging session the RG cell divided at the ventricular surface to produce a presumptive IPCs, that went on to divide in the SVZ (Figure 1D). The expression of basic helix-loop-helix (bHLH) transcription factors is required for the specification of cortical interneuron progenitors (Petryniak et al., 2007). Therefore, we examined bHLH transcription factor expression in cells located in the SVZ of the MGE 48 h after *in utero* infection. We found that a majority of GFP positive cells (85%, n=3 brains, 134 cells) coexpressed the ventral telencephalic progenitor markers Olig2 (20.8%), Mash1 (29.9%), or both (34.3%) (Casarosa et al., 1999; Petryniak et al., 2007) (Figure 1E, and Figures S1 and S2). We also characterized the pattern of cell division of IPCs in the SVZ of the MGE using time-lapse microscopy (Figure 1F). We observed 13 divisions of SVZ progenitors, each producing two cells with the bipolar morphology of migrating neurons. During one imaging session, we observed SVZ cells undergoing division to produce two daughter cells that each divided again, resulting in four neuronal progeny (Movie S1). This suggests that IPC divisions contribute to the expansion of neuronal lineages in the MGE similar to the way they contribute to neurogenesis in the dorsal telencephalon (Lui et al., 2011; Noctor et al., 2004; Vasistha et al., 2014).

A previous study suggested that clonal relationships might regulate the clustering or distribution of sibling interneurons (Brown et al., 2011). This suggestion raises the possibility that migration of sibling cells may be coordinated. We found that 2–8 h after birth, pairs of sibling neurons (n=8) rapidly migrated in multiple directions independent of each other (Movie S1), consistent with previous studies reporting that the trajectories of newborn neurons in the MGE mantle zone vary randomly (Tanaka et al., 2009). It was not possible to simultaneously track the movement of sibling cells to their final positions due to the distances and speed at which they migrated (Movie S1).

To address the possibility that sibling cells may be intrinsically programmed to reach the same cortical destination, we sought a method whereby clonal progeny could be distinguished in the mature cortex. We were able to specifically label MGE progenitors through the combined use of transgenic mice and retroviral vectors so that only MGE progenitors would be infected. We utilized a genetically modified Replication Competent ASLV long terminal repeat with Splice Acceptor (RCAS) viral vector, combined with

transgenic expression of the RCAS cognate receptor TVA in cells of the ganglionic eminence (Figure 2A). Under normal conditions, RCAS vectors are only able to infect avian cells (Young et al., 1993). However, the use of transgenic mice that express the cognate TVA receptor enables the virus to infect mammalian cells (Brown et al., 2011; von Werder et al., 2012). We used two mutant mouse lines to express TVA in ventral telencephalic progenitors: Olig2-Tva-ires-Cre, in which Tva-ires-cre is knocked into the Olig2 locus, and Nkx2.1-Cre;LSL-Tva lines (Brown et al., 2011; Schuller et al., 2008; von Werder et al., 2012; Xu et al., 2008) (Figure 2A, Figure S3). We were able to achieve specific and sparse labeling of progenitors in the ganglionic eminences with *in utero* intraventricular injection of a recombinant GFP-expressing RCAS virus, and confirmed that the injection of RCAS into both TVA lines at E12.5 resulted in specific labeling of interneurons in the mature brain (Figure 2B and 2C and Figure S3). Most GFP positive cells co-labeled with the interneuron subtype markers PV and SOM (53.0% and 24.0% respectively, n=4 brains, 701 cells) (Figure 2D). We chose to focus the rest of our analysis on the Nkx2.1-Cre; LSL-Tva line because infection was confined to MGE progenitors instead of all ventral telencephalic progenitors, as in the Olig2-Tva-Cre line (Figure S3A–C).

Upon *in utero* intraventricular injection of RCAS-GFP into E12.5 Nkx2.1-Cre; LSL-Tva mice, we observed clustering of cortical interneurons in both the mature and developing cortex, consistent with previous reports of clustering of sparse virus labeled neurons (Brown et al., 2011; Ciceri et al., 2013) (Figure 2E and 2F). We reasoned that if sibling cells were clustered, we should observe segregation and/or aggregation of virus labeled cells derived from a common progenitor. To this end, we injected E12.5 embryos from Nkx2.1-Cre;LSL-Tva mice with a mixture of RCAS-GFP:RCAS-mCherry viruses (Figure 2G). Our rationale was that we would observe clusters of GFP and mCherry positive clonally related clusters dispersed throughout the brain. We harvested the injected brains at P28 and found numerous examples of cell clusters consisting of red, green, and yellow cells (Figure 2H). We then measured the cumulative nearest neighbor distribution between cells of the same or different color (Figure 2I). We found that different color neighbors were more closely distributed than cells of the same color ($p < 0.01$, n=3 brains, 234 cells), suggesting that clustering can occur independently of lineage. However, the true distribution of cells in relation to their clonal siblings cannot be determined with this method because clustered cells sharing the same color could be derived from different progenitors.

To directly determine the clonal relationship of clustered interneurons, we utilized an EnvA-pseudotyped retrovirus library carrying oligonucleotide sequence tags or barcodes (Cepko et al., 1995; Fuentealba et al., 2015; Jiang et al., 2013; Walsh and Cepko, 1992) (Figure 3A). In addition to the barcode sequence, each virus contained a transgene for membrane-bound GFP. The retroviral library, consisting of 10^5 unique 24-base pair barcode sequences, was injected *in utero* into the lateral ventricle of E12.5 Nkx2.1-cre;LSL-Tva embryos at a concentration between 5×10^7 and 5×10^5 cfu/ml (Figure 3B). Brains of infected transgenic mice were harvested at P28 and sectioned and stained for interneuron subtype markers PV and SOM. The position of each cell and its histological subtype was then recorded (Table S1). In order to determine the barcode sequence, each mapped cell was collected by laser capture microdissection, and the viral tag amplified by nested PCR and sequenced (Figure

3C–E). The clonal, histological, and spatial information was then combined to build three-dimensional maps of GFP positive cells in the brains of P28 mice (Figure 3F). In order to control for contamination and screen for viral silencing, we randomly collected and PCR amplified GFP negative pieces of tissue for every GFP positive cell. A very small number of barcodes were detected from GFP negative tissue (< 1%, n=701 cells). Between 14 and 234 cells were labeled from each injection (n = 8 hemispheres, 4 brains). Given the number of cells infected in each hemisphere, the probability of neurons containing the same tag arising from two independent progenitor infections is exceedingly low (Cepko et al., 1995; Jiang et al., 2013; Walsh and Cepko, 1992). Therefore, multiple cells sharing the same barcode are presumed to be clonally related siblings.

Amplified and sequenced barcodes were obtained from 302 cells, 30.1% of which were part of a multi-cell clone, defined as two or more cells sharing the same barcode. The majority of individual cells (69.9%) carried unique barcodes, indicating that either they were single cell clones, or we failed to amplify the barcode of their sibling cells. The average size of multi-cell clones was 2.8 cells, with the largest clones containing 6 cells (Figure 4A). Neurons that returned barcode sequence tags were widely dispersed across multiple forebrain structures including the amygdala, cortex, hippocampus and striatum, with the majority located in the cortex (66.2%, n=302) (Figure 4B). We never observed clonal siblings in different hemispheres, or mixed clones consisting of neurons and glia (data not shown). When we examined the composition of multi-cell clones, we found that nearly 30% consisted of a mixture of PV and SOM subtypes, while fewer than 30% were positive for a single marker, and 20% were negative for both markers (Figure 4A and 4C). We were unable to discern a predominant composition of mixed subtype clones, as we observed clones with either PV⁺ or SOM⁺ cells as a major component (Figure 4A and Figure S5A–B).

When examining the spatial distribution of multi-cell clones, we observed that sibling neurons were widely dispersed across different brain structures. Most cells were located hundreds or thousands of microns from their nearest identified sibling cell (Figure 4A and 4D). The only observed pair of clonally related cells located in the same 25µm thick brain section was a pair of glia in the septum, consistent with previous findings of local proliferation of glial progenitor cells (Figure 4D, Clone 16) (Ge et al., 2012). We examined the nearest neighbor distribution of retrovirus labeled GFP positive cells by assigning coordinates to each cell during serial section reconstruction and categorizing cells as sibling members of a multi-cell clone, unrelated clones, or cells that did not return a barcode sequence (unknown lineage) (Figure 4D and Table S1). The average distance between siblings was substantially larger than that of unrelated clones. A substantial portion of multi-cell cortical clones had at least one sibling cell located in a different forebrain structure (42.1%, n= 3 brains); while the remainder of clones were confined to the cortex. We plotted the NND of all cells, regardless of category, and compared them to 100 computer simulations of randomly distributed neurons (Figure 4E). We found that between approximately 250–500µm in NND there were significant differences in the spatial organization of our experimental dataset when compared to randomized simulations (n= 284 cells), suggesting that the overall population distribution is not random, consistent with previous studies (Brown et al., 2011). Next we compared the NND cortical siblings to unrelated cortical clones. We found the NND of cortical sibling clones to have a

significantly wider dispersion than unrelated clones (mean 750 μ m vs 585 μ m respectively, $p = 0.01$, $n=2$ hemispheres, 216 cells) (Figure 4E), suggesting that more closely clustered cells are derived from independent clonal lineages. Taken together, our findings suggest that MGE interneurons derived from a common progenitor, are widely dispersed across different regions of the brain, and that the majority of clustered cells observed with sparse viral labeling are likely not clonally-related.

Discussion

Using retroviral fate mapping and genetic tagging, we followed the development of cortical interneurons to understand the role of clonal relationships in regulating their integration into functional circuitry. Ventral telencephalic RG appear to be the primary neural stem cells, dividing asymmetrically to produce IPCs that subsequently divide symmetrically to expand their numbers, or more frequently, to produce pairs of neurons. These findings suggest significant similarities in the patterns of cell division in the dorsal and ventral regions of the telencephalon. However, there are possible differences in cell cycle dynamics, proliferative potential, and relative proportions of progenitor subtypes which likely lead to differences in SVZ organization and the number of cells produced in each region (Pilz et al., 2013). The developmental history of clonally-related cells in the cortex and MGE diverges significantly once postmitotic neurons are produced. Newborn excitatory neurons derived from the same clonal lineage in the cortex migrate along RG and generally remain closely associated. These neurons remain vertically aligned in the developing rodent brain, allowing them to have continuous contact with their siblings (Noctor et al., 2001). In contrast, newborn inhibitory interneurons are highly motile and do not appear to maintain an association with their sibling cells. The long distances inhibitory neurons must migrate to reach their target region may preclude the development of sustained connectivity between related cells, and may necessitate alternative strategies for circuit organization independent of lineage relationships.

Dispersion of Clonally Related Interneurons

There has been significant interest in the role that clonal relationships might play in the organization of cortical neurons. It has been previously suggested that clonal identity could influence the connectivity of sibling cells within cortical circuits (Li et al., 2012; Sultan et al., 2014; Yu et al., 2012). The clustered appearance of radially and horizontally aligned interneurons following sparse viral labeling is visually striking and appears to support the idea that clonal relationships dictate these alignments (Brown et al., 2011; Ciceri et al., 2013). However, we consistently found that interneuron clones were widely dispersed throughout different forebrain regions, and that clustered cells were clonally distinct, suggesting that interneuron clusters observed following sparse retroviral labeling are largely composed of unrelated cells (Figure 5). What are the possible reasons for the discrepancy between our interpretation and those of previous studies? The key methodological difference is our use of large numbers of tags to differentiate cells derived from separate clonal lineages. Utilizing a sufficiently complex library of tags is necessary to prevent erroneous assignment of clonal relationships between cells based only on their proximity. This is especially important when tracing the lineage of cells with a broad migratory capacity such

as those derived from the MGE. Two previous studies utilized either one or two markers to differentiate cells of different lineages, and it's worth noting that even when utilizing two fluorescent tags for sparse labeling, Ciceri and colleagues observed mixing of the two labels in over half of their clusters (Ciceri et al, 2013).

Technical Considerations for Lineage Tracing with Barcodes

Retroviral barcode libraries provide a powerful method for determining lineage relationships in populations of cells regardless of their pattern of migration, but this method has limitations related to gene silencing and cell death. Silencing of the retroviral reporter may be a factor contributing to the reduced clone size we observed in our analysis. We attempted to survey for silencing by random laser-capture microdissection of GFP negative tissue. However, given the wide dispersion of clonal cells, our random cell collections likely yielded an underestimate of silencing. Studies using the same retroviral reporter used here and systematically examining silencing across large areas of GFP negative brain tissue found that silencing can account for some reduction in clone size, but notably did not uncover a consistent pattern of silencing (Mayer et al. submitted). Consistent with previous studies using retroviral barcode libraries, we recovered tags from only a portion of labeled cells - 43% of GFP positive cells (302 out of 701) - a limitation that can also affect determination of clone size and composition (Reid and Walsh, 2002). While these factors prevent us from drawing conclusions about the true size of the clones or their complete pattern of composition, we do not believe this affects our interpretation. To our knowledge retroviral silencing is a random event, so if sibling clustering were a dominant mechanism for organization we would expect some portion of our multi-cell clones to be clustered. However, nearly all of our clonally related cells were widely dispersed, and we observed clustering of unrelated cells. As mentioned above, we sampled a piece of GFP negative tissue for every cell collected typically within the same field of view as the GFP positive cell. On the rare occasions when we amplified tags from GFP negative tissue, the barcode never matched the GFP positive cell that was nearby. Our findings support the idea that clonal lineage is not the primary determinant for spatial aggregation of MGE-derived interneurons. Our data also suggest that spatial and temporal origin may influence clustering. Nonetheless, we cannot rule out the possibility that a small subpopulation of clonally related cells could be clustered.

In our study, we focused on the distribution of clones in the P28 mouse brain, past the period of cortical interneuron cell death (Southwell et al., 2010). It is therefore possible that intrinsically determined cell death could play a role in regulating the distribution and composition of interneuron clones. However, it seems unlikely that the pattern of apoptosis has significantly distorted our observed clonal relationships, since similar clusters of sparse retroviral labeled interneurons have been observed both before and after the peak period of cell death (Brown et al., 2011; Ciceri et al., 2013). The demonstration that clusters include unrelated cells indicates that a mechanism other than lineage contributes to clustering, regardless of a possible role of cell death.

Spatial and Temporal Regulation of Neuronal Organization

How can independently generated, non-related neurons arrive at the same cortical site? One possibility is that the spatial and temporal origin of interneurons might play an instructive role in determining their final position (Ciceri et al., 2013; Marin and Muller, 2014). This possibility raises the question of whether spatial and temporal identities might also dictate circuit relationships between cortical interneurons.

While functionally and histologically distinct PV and SOM interneuron subtypes are both derived from the MGE (Kepecs and Fishell, 2014), it has been unclear whether they derive from distinct or common progenitor lineages. Our observation that the majority of multi-cell clones consisted of both SOM and PV subtypes, suggests that at E12.5 single MGE progenitors generate multiple neuronal subtypes. This has important implications for understanding the cellular mechanisms regulating cell fate determination. Distinct neuronal subtypes might be generated within a single clone in a specific temporal pattern. A temporal pattern of neural subtype production occurs in invertebrates and also in clones of excitatory neurons where deep layer subcortical projection neurons are produced first, followed by superficial layer callosal projection neurons (Bayraktar and Doe, 2013; Kohwi and Doe, 2013; Leone et al., 2008). Alternatively, two sibling cells sharing the same birthdate could have different cell fates, as has been shown in the retina where intermediate progenitors produce two daughter cells with distinct postmitotic cell fates (Cepko, 2014). Intermediate progenitor cells in the MGE could similarly generate daughter cells of different cell subtypes. Further studies will be necessary to determine the subtype identity of the daughters of IPC divisions in the MGE.

Materials and Methods

Retrovirus Production and In utero Injections

Replication-incompetent GFP-expressing retrovirus was produced from a stably transfected packaging line and injected into E12.5 gestation stage pregnant mice, as previously reported (Noctor et al., 2001).

Immunostaining and Laser-Microdissection Microscopy

Mice were sacrificed and their brains were processed for immunohistochemistry as previously described. Floating sections (25 μm) were stained with the following primary antibodies: chicken anti-GFP (1:750, Aves Lab) rabbit anti-somatostatin (Millipore, 1:750); mouse anti-parvalbumin (Millipore 1:1000). Secondary antibodies used were: Alexafluor 488 (1:1000), 546 (1:500), or 647 (1:500) conjugated donkey anti-mouse, anti-rabbit or goat (Life Technologies). Sections were mounted in PEN-membrane slides (2 μm , JH Technologies). Individual labeled cells were mapped and laser-microdissected with small amount of surrounding tissue (4000–6000 μm^2), using a Zeiss PALM MicroBeam LCM (v4.3.2.13, Carl Zeiss MicroImaging). GFP-negative control tissue was also dissected for every positive dissection. Dissected tissue was collected in 20 μl of Proteinase K solution (20 $\mu\text{g}/\text{ml}$ proteinase K (Roche), 50mM TrisHCl pH 7.5, 50mM KCl, 2.5mM MgCl₂, and 0.5% Igepal CA-630 (Sigma)) and incubated for 2 h at 60°C, followed by 20 min at 85°C and 10 min at 95°C. The first round of PCR “barcode” amplification was done by adding 40

μl of 1st PCR mix that included Platinum® Pfx DNA Polymerase (Life Technologies) and primers SBR161 (5'-GACAACCACTACCTGAGCACCCAGT-3') and SBR126 (5'-GGCTCGTACTCTATAGGCTTCAGCTGGTGA-3'). The 2nd PCR mix included 2 μl of the 1st PCR reaction, Platinum® Pfx DNA Polymerase, and primers SBR160 (5'-ATCACATGGTCTGCTGGAGTTCGTGA-3') and SBR128 (5'-ATTGTTGAGTCAAACTAGAGCCTGGACCA-3') to a total of 20 μl . PCR products were cleaned and sequenced using primer SB160. After identification of clones, the positions of selected positive cells were reconstructed in 3D images using NeuroLucida® (v10.31 MBF Biosciences-MicroBrightField Inc.).

Brain sectioning, cortical slice culture, viral infection on slice and timelapse imaging

Retrovirus infected brains were vibratome-sliced cultured and imaged as previously described (Noctor et al., 2001).

Statistical Analysis

GFP positive cells were assigned coordinates from serial section reconstructions using NeuroLucida. After determining the distance between each interneuron and the closest one, we compared these distances to the values expected for a sample of neurons located at random in the same volume. Specifically, for each experiment, the experimental interneuron distribution was compared with 100 simulated distributions, generated by positioning the same number of elements at random locations distributed uniformly in the exact same region of tissue as the experimental condition. NNDs were displayed as cumulative distributions.

Supplementary Material

Refer to Web version on PubMed Central for supplementary material.

Acknowledgements

We would like to thank William Walantus and Yingying Wang for technical assistance with *in utero* viral injections and histology. We thank members of the Alvarez-Buylla, Rowitch and Kriegstein labs for ideas arising from numerous critical discussions. We are extremely grateful to Rebecca Ihrie for providing brain atlas tracings. This project was supported by NIH R01NS035710 to ARK, and NIH R37HD032116 to AAB.

References

- Anderson SA, Kaznowski CE, Horn C, Rubenstein JL, McConnell SK. Distinct origins of neocortical projection neurons and interneurons in vivo. *Cerebral cortex*. 2002; 12:702–709. [PubMed: 12050082]
- Anderson SA, Marín O, Horn C, Jennings K, Rubenstein JL. Distinct cortical migrations from the medial and lateral ganglionic eminences. *Development*. 2001; 128:353–363. [PubMed: 11152634]
- Bayraktar OA, Doe CQ. Combinatorial temporal patterning in progenitors expands neural diversity. *Nature*. 2013; 498:449–455. [PubMed: 23783519]
- Brown KN, Chen S, Han Z, Lu C-H, Tan X, Zhang X-J, Ding L, Lopez-Cruz A, Saur D, Anderson SA, et al. Clonal production and organization of inhibitory interneurons in the neocortex. *Science*. 2011; 334:480–486. [PubMed: 22034427]
- Butt SJ, Sousa VH, Fuccillo MV, Hjerling-Leffler J, Miyoshi G, Kimura S, Fishell G. The requirement of Nkx2-1 in the temporal specification of cortical interneuron subtypes. *Neuron*. 2008; 59:722–732. [PubMed: 18786356]

- Butt SJB, Fuccillo M, Nery S, Noctor S, Kriegstein A, Corbin JG, Fishell G. The temporal and spatial origins of cortical interneurons predict their physiological subtype. *Neuron*. 2005; 48:591–604. [PubMed: 16301176]
- Casarosa S, Fode C, Guillemot F. Mash1 regulates neurogenesis in the ventral telencephalon. *Development*. 1999; 126:525–534. [PubMed: 9876181]
- Cepko C. Intrinsically different retinal progenitor cells produce specific types of progeny. *Nature reviews Neuroscience*. 2014; 15:615–627. [PubMed: 25096185]
- Cepko C, Ryder EF, Austin CP, Walsh C, Fekete DM. Lineage analysis using retrovirus vectors. *Methods in enzymology*. 1995; 254:387–419. [PubMed: 8531701]
- Ciceri G, Dehorter N, Sols I, Huang ZJ, Maravall M, Marin O. Lineage-specific laminar organization of cortical GABAergic interneurons. *Nature neuroscience*. 2013; 16:1199–1210. [PubMed: 23933753]
- Fuentealba LC, Rompani SB, Parraguez JI, Obernier K, Romero R, Cepko CL, Alvarez-Buylla A. Embryonic Origin of Postnatal Neural Stem Cells. *Cell*. 2015; 161:1644–1655. [PubMed: 26091041]
- Ge WP, Miyawaki A, Gage FH, Jan YN, Jan LY. Local generation of glia is a major astrocyte source in postnatal cortex. *Nature*. 2012; 484:376–380. [PubMed: 22456708]
- Hansen DV, Lui JH, Parker PR, Kriegstein AR. Neurogenic radial glia in the outer subventricular zone of human neocortex. *Nature*. 2010; 464:554–561. [PubMed: 20154730]
- Haubensak W, Attardo A, Denk W, Huttner WB. Neurons arise in the basal neuroepithelium of the early mammalian telencephalon: a major site of neurogenesis. *Proceedings of the National Academy of Sciences of the United States of America*. 2004; 101:3196–3201. [PubMed: 14963232]
- Jiang H, Wang L, Beier KT, Cepko CL, Fekete DM, Brigande JV. Lineage analysis of the late otocyst stage mouse inner ear by transuterine microinjection of a retroviral vector encoding alkaline phosphatase and an oligonucleotide library. *PLoS one*. 2013; 8:e69314. [PubMed: 23935981]
- Kepecs A, Fishell G. Interneuron cell types are fit to function. *Nature*. 2014; 505:318–326. [PubMed: 24429630]
- Kohwi M, Doe CQ. Temporal fate specification and neural progenitor competence during development. *Nature reviews Neuroscience*. 2013; 14:823–838. [PubMed: 24400340]
- Leone DP, Srinivasan K, Chen B, Alcamo E, McConnell SK. The determination of projection neuron identity in the developing cerebral cortex. *Current opinion in neurobiology*. 2008; 18:28–35. [PubMed: 18508260]
- Li Y, Lu H, Cheng PL, Ge S, Xu H, Shi SH, Dan Y. Clonally related visual cortical neurons show similar stimulus feature selectivity. *Nature*. 2012; 486:118–121. [PubMed: 22678292]
- Lui JH, Hansen DV, Kriegstein AR. Development and evolution of the human neocortex. *Cell*. 2011; 146:18–36. [PubMed: 21729779]
- Marin O. Cellular and molecular mechanisms controlling the migration of neocortical interneurons. *The European journal of neuroscience*. 2013; 38:2019–2029. [PubMed: 23651101]
- Marin O, Muller U. Lineage origins of GABAergic versus glutamatergic neurons in the neocortex. *Current opinion in neurobiology*. 2014; 26:132–141. [PubMed: 24549207]
- Miller FD, Gauthier AS. Timing is everything: making neurons versus glia in the developing cortex. *Neuron*. 2007; 54:357–369. [PubMed: 17481390]
- Miyoshi G, Butt SJB, Takebayashi H, Fishell G. Physiologically distinct temporal cohorts of cortical interneurons arise from telencephalic Olig2-expressing precursors. *The Journal of neuroscience : the official journal of the Society for Neuroscience*. 2007; 27:7786–7798. [PubMed: 17634372]
- Nery S, Fishell G, Corbin JG. The caudal ganglionic eminence is a source of distinct cortical and subcortical cell populations. *Nature neuroscience*. 2002; 5:1279–1287. [PubMed: 12411960]
- Nobrega-Pereira S, Kessaris N, Du T, Kimura S, Anderson SA, Marin O. Postmitotic Nkx2-1 controls the migration of telencephalic interneurons by direct repression of guidance receptors. *Neuron*. 2008; 59:733–745. [PubMed: 18786357]
- Noctor SC, Flint AC, Weissman TA, Dammerman RS, Kriegstein AR. Neurons derived from radial glial cells establish radial units in neocortex. *Nature*. 2001; 409:714–720. [PubMed: 11217860]

- Noctor SC, Martínez-Cerdeño V, Ivic L, Kriegstein AR. Cortical neurons arise in symmetric and asymmetric division zones and migrate through specific phases. *Nature neuroscience*. 2004; 7:136–144. [PubMed: 14703572]
- Petryniak MA, Potter GB, Rowitch DH, Rubenstein JLR. Dlx1 and Dlx2 control neuronal versus oligodendroglial cell fate acquisition in the developing forebrain. *Neuron*. 2007; 55:417–433. [PubMed: 17678855]
- Pilz GA, Shitamukai A, Reillo I, Pacary E, Schwausch J, Stahl R, Ninkovic J, Snippert HJ, Clevers H, Godinho L, et al. Amplification of progenitors in the mammalian telencephalon includes a new radial glial cell type. *Nature communications*. 2013; 4:2125.
- Rakic P. Specification of cerebral cortical areas. *Science*. 1988; 241:170–176. [PubMed: 3291116]
- Reid CB, Walsh CA. Evidence of common progenitors and patterns of dispersion in rat striatum and cerebral cortex. *The Journal of neuroscience : the official journal of the Society for Neuroscience*. 2002; 22:4002–4014. [PubMed: 12019320]
- Schuller U, Heine VM, Mao J, Kho AT, Dillon AK, Han YG, Huillard E, Sun T, Ligon AH, Qian Y, et al. Acquisition of granule neuron precursor identity is a critical determinant of progenitor cell competence to form Shh-induced medulloblastoma. *Cancer cell*. 2008; 14:123–134. [PubMed: 18691547]
- Southwell DG, Froemke RC, Alvarez-Buylla A, Stryker MP, Gandhi SP. Cortical plasticity induced by inhibitory neuron transplantation. *Science*. 2010; 327:1145–1148. [PubMed: 20185728]
- Sultan KT, Shi W, Shi SH. Clonal origins of neocortical interneurons. *Current opinion in neurobiology*. 2014; 26:125–131. [PubMed: 24531366]
- Tanaka DH, Yanagida M, Zhu Y, Mikami S, Nagasawa T, Miyazaki J, Yanagawa Y, Obata K, Murakami F. Random walk behavior of migrating cortical interneurons in the marginal zone: time-lapse analysis in flat-mount cortex. *The Journal of neuroscience : the official journal of the Society for Neuroscience*. 2009; 29:1300–1311. [PubMed: 19193877]
- Tricoire L, Pelkey KA, Erkkila BE, Jeffries BW, Yuan X, McBain CJ. A blueprint for the spatiotemporal origins of mouse hippocampal interneuron diversity. *The Journal of neuroscience : the official journal of the Society for Neuroscience*. 2011; 31:10948–10970. [PubMed: 21795545]
- Vasistha NA, Garcia-Moreno F, Arora S, Cheung AF, Arnold SJ, Robertson EJ, Molnar Z. Cortical and Clonal Contribution of Tbr2 Expressing Progenitors in the Developing Mouse Brain. *Cerebral cortex*. 2014
- von Werder A, Seidler B, Schmid RM, Schneider G, Saur D. Production of avian retroviruses and tissue-specific somatic retroviral gene transfer in vivo using the RCAS/TVA system. *Nature protocols*. 2012; 7:1167–1183. [PubMed: 22635109]
- Walantus W, Castaneda D, Elias L, Kriegstein A. In utero intraventricular injection and electroporation of E15 mouse embryos. *J Vis Exp*. 2007; 239
- Walsh C, Cepko CL. Widespread dispersion of neuronal clones across functional regions of the cerebral cortex. *Science*. 1992; 255:434–440. [PubMed: 1734520]
- Wang X, Tsai JW, LaMonica B, Kriegstein AR. A new subtype of progenitor cell in the mouse embryonic neocortex. *Nature neuroscience*. 2011; 14:555–561. [PubMed: 21478886]
- Wonders CP, Anderson SA. The origin and specification of cortical interneurons. *Nature reviews Neuroscience*. 2006; 7:687–696. [PubMed: 16883309]
- Xu Q, Cobos I, De La Cruz E, Rubenstein JL, Anderson SA. Origins of cortical interneuron subtypes. *The Journal of neuroscience : the official journal of the Society for Neuroscience*. 2004; 24:2612–2622. [PubMed: 15028753]
- Xu Q, Tam M, Anderson SA. Fate mapping Nkx2.1-lineage cells in the mouse telencephalon. *The Journal of comparative neurology*. 2008; 506:16–29. [PubMed: 17990269]
- Young JA, Bates P, Varmus HE. Isolation of a chicken gene that confers susceptibility to infection by subgroup A avian leukosis and sarcoma viruses. *J Virol*. 1993; 67:1811–1816. [PubMed: 8383211]
- Yu Y-C, Bultje RS, Wang X, Shi S-H. Specific synapses develop preferentially among sister excitatory neurons in the neocortex. *Nature*. 2009; 458:501–504. [PubMed: 19204731]
- Yu YC, He S, Chen S, Fu Y, Brown KN, Yao XH, Ma J, Gao KP, Sosinsky GE, Huang K, et al. Preferential electrical coupling regulates neocortical lineage-dependent microcircuit assembly. *Nature*. 2012; 486:113–117. [PubMed: 22678291]

Highlights

1. Cortical interneurons derive from symmetric divisions of intermediate progenitors.
2. Histologically distinct interneuron subtypes derive from the same clonal lineage.
3. Clonally related interneurons are widely dispersed.

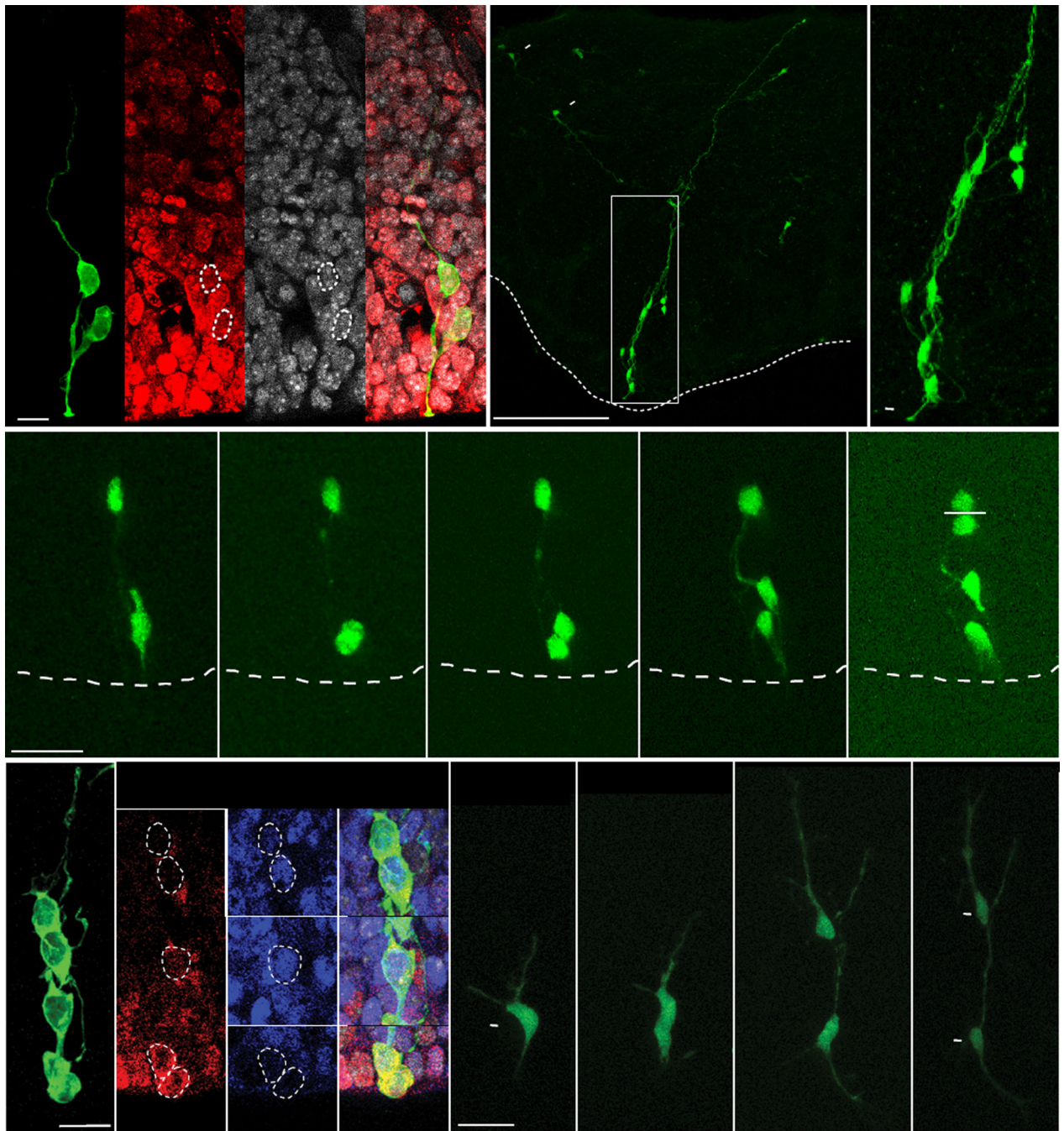


Figure 1. MGE Progenitors are Arranged in Radial Arrays of Clonally Related Cells
 (A) 24 h after injection we observed a single radial glial cell and its progeny. Both the RG cell and progeny were positive for the proliferative cell marker Ki67. (B) Radial arrays of cells in the mouse MGE approximately 90 h after injection with a GFP-expressing retrovirus. Neurons are also observed migrating tangentially away from the clone (arrowhead). (C) Higher magnification view of the clone identifies 8 anatomically associated cells, one being a radial glial cell with an apical endfoot (arrowhead) attached to the ventricular surface. (D) Time-lapse imaging of a radial glial cell in the MGE shows an

asymmetrical radial glial cell division at the ventricular surface that produces an IPC, and also a previously generated IPC dividing in the SVZ. (E) Retroviral GFP labeled MGE progenitors 48 h after viral infection. Non-radial glial progeny express bHLH transcription factors Mash1 (blue) and Olig2 (red) n= 134. (F) Time-lapse imaging of an E13.5 embryonic mouse organotypic slice shows a GFP+ IPC dividing to produce a pair of neuronal progeny. Scale bars: (A) 15 μ m, (B) 300 μ m, (D) 25 μ m, (E and F) 20 μ m.

Author Manuscript

Author Manuscript

Author Manuscript

Author Manuscript

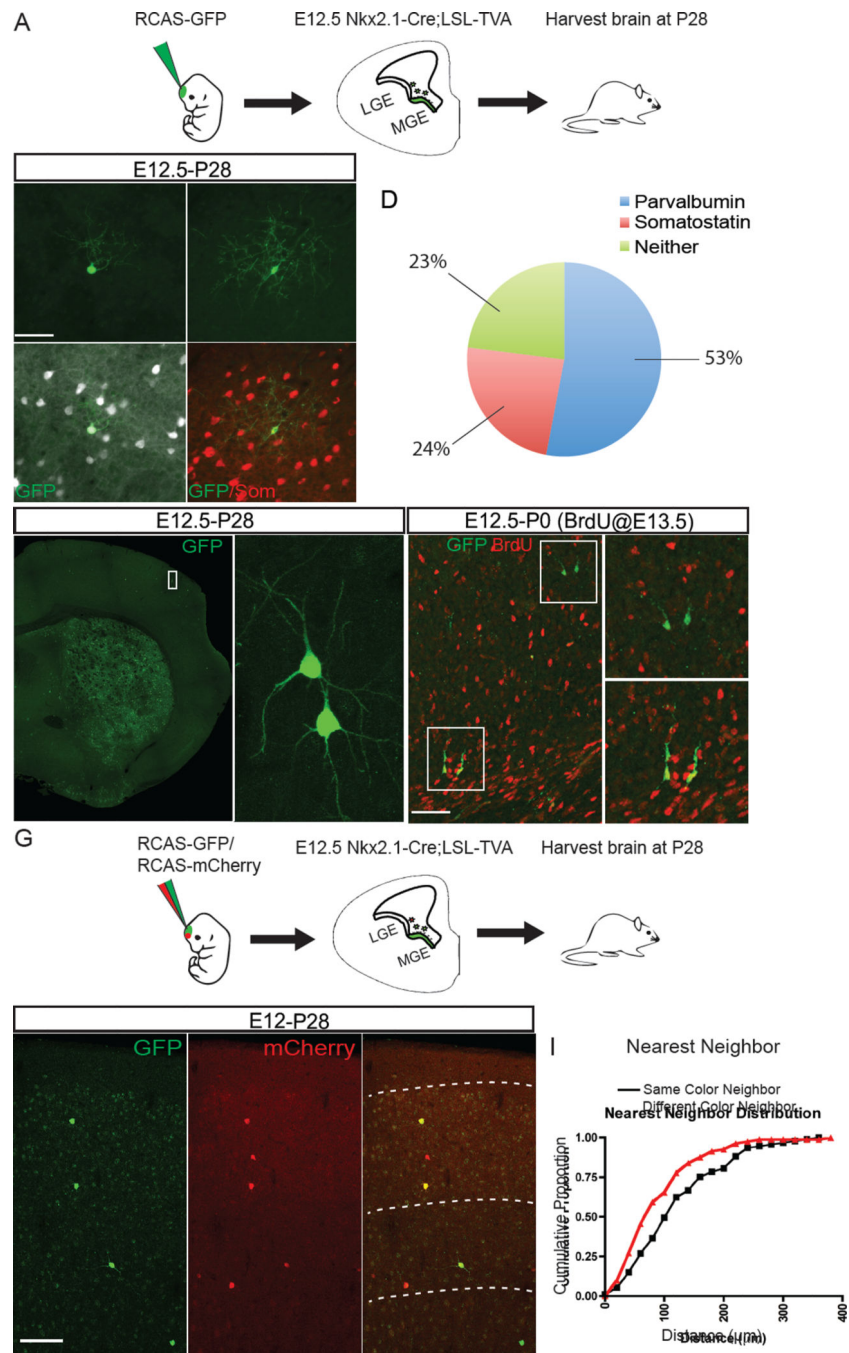


Figure 2. Clustering of Sparsely Labeled Medial Ganglionic Eminence Progenitors
 (A) E12.5 Nkx2.1-Cre;LSL-Tva mouse embryo showing the TVA⁺ region of the MGE progenitor zone where RCAS viral infection is permitted in green. (B–C) P28 brain sections containing RCAS-GFP virus labeled clones stained with parvalbumin (white) (B and B') or somatostatin (red) (C, and C'). (D) Pie chart showing the percentage of cells positive for parvalbumin (PV), somatostatin (SOM), or negative for both markers (Neither) from Nkx2.1-Cre;LSL-Tva injected brains (n= 4 brains, 701 cells). (E) Coronal section of P28 mouse brain injected with RCAS-EGFP virus at E12.5. Sparse EGFP⁺ neurons appear to

cluster together into groups of two or more cells. (F) RCAS-EGFP labeled neurons, derived from infections of progenitors in the developing cortex with a, BrdU pulse given 24 h after infection (red), showing that EGFP+ neighboring cells often share the same BrdU labeling status. The upper box shows a pair of BrdU- migratory neurons (upper magnified panel), whereas the lower box shows a pair of BrdU+ migratory neurons (lower magnified panel). (G) E12.5 Nkx2.1-Cre;LSL-Tva mouse embryos injected with a mixture of RCAS-GFP and RCAS-mCherry viruses and harvested at P28. (H) Coronal sections of mice injected with mixed virus showing clusters of red, green and yellow cells. (I) Cumulative proportion of nearest neighbor distribution (NND) of same (black) and different (red) fluorophores (n=3 brains n=215 cells, $p < 0.01$, Kolmogorov-Smirnov). Scale bars: (B) 50 μ m, (G) 100 μ m.

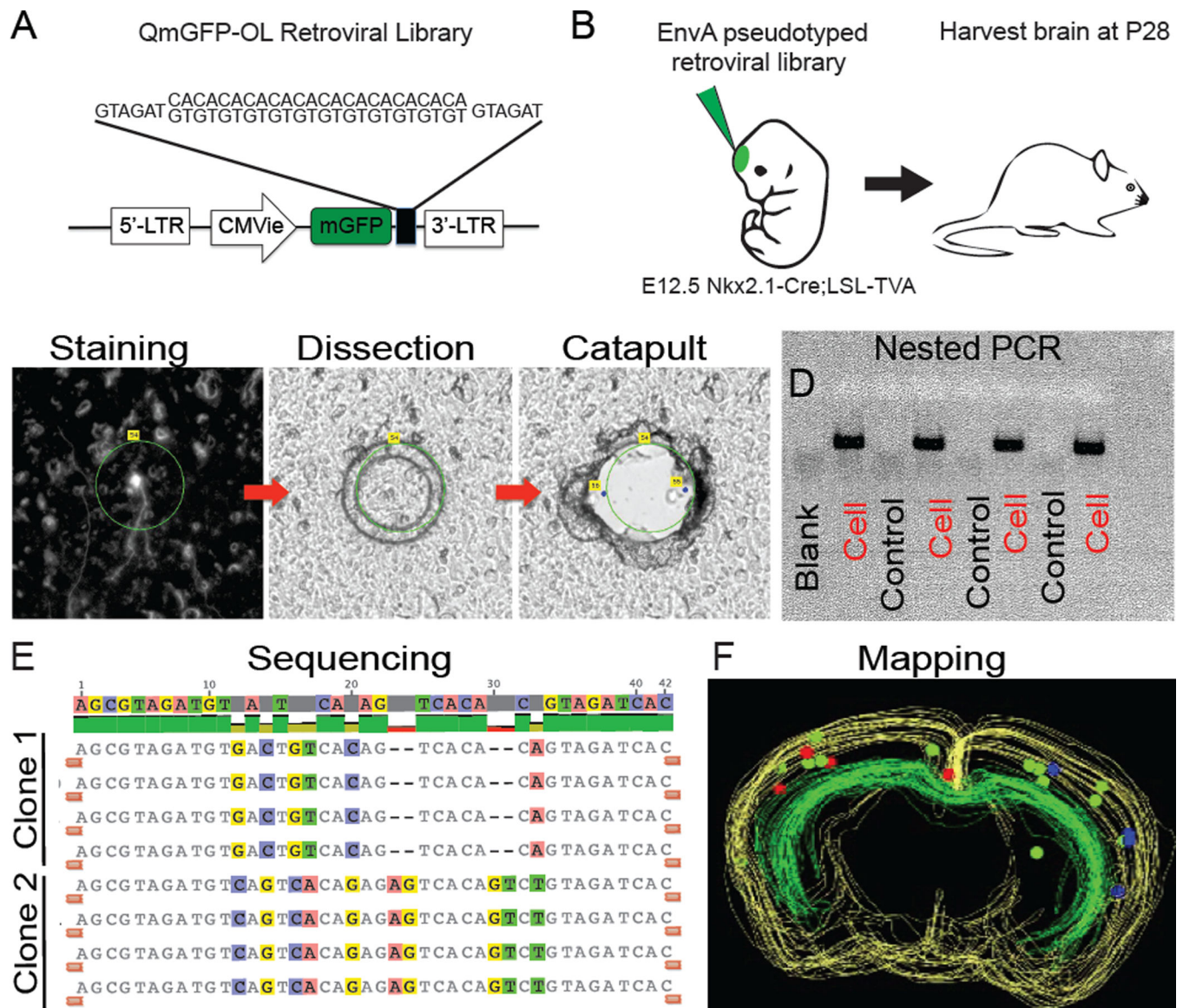


Figure 3. Lineage Analysis of Nkx2.1+ Progenitors Using Barcode Retroviral Library
 (A) Schematic of the QmGFP-OL murine retroviral library. Each retrovirus expresses membrane GFP and contains a 24 bp barcode sequence. (B) EnvA pseudotyped retrovirus libraries were intraventricularly delivered into Nkx2.1-Cre;LSL-Tva embryos at E12.5; brains were harvested and analyzed at P28. (C) Stained neuron outlined for laser capture microdissection and catapulting. (D) Example gel of nested PCR products of dissected cells and GFP negative tissue sections used as controls. (E) Example barcode sequence alignment showing two four-cell clones with matching barcodes. (F) Three dimensional map of two four-cell clones shown in red and blue. Green spheres show cells which did not return a barcode sequence.

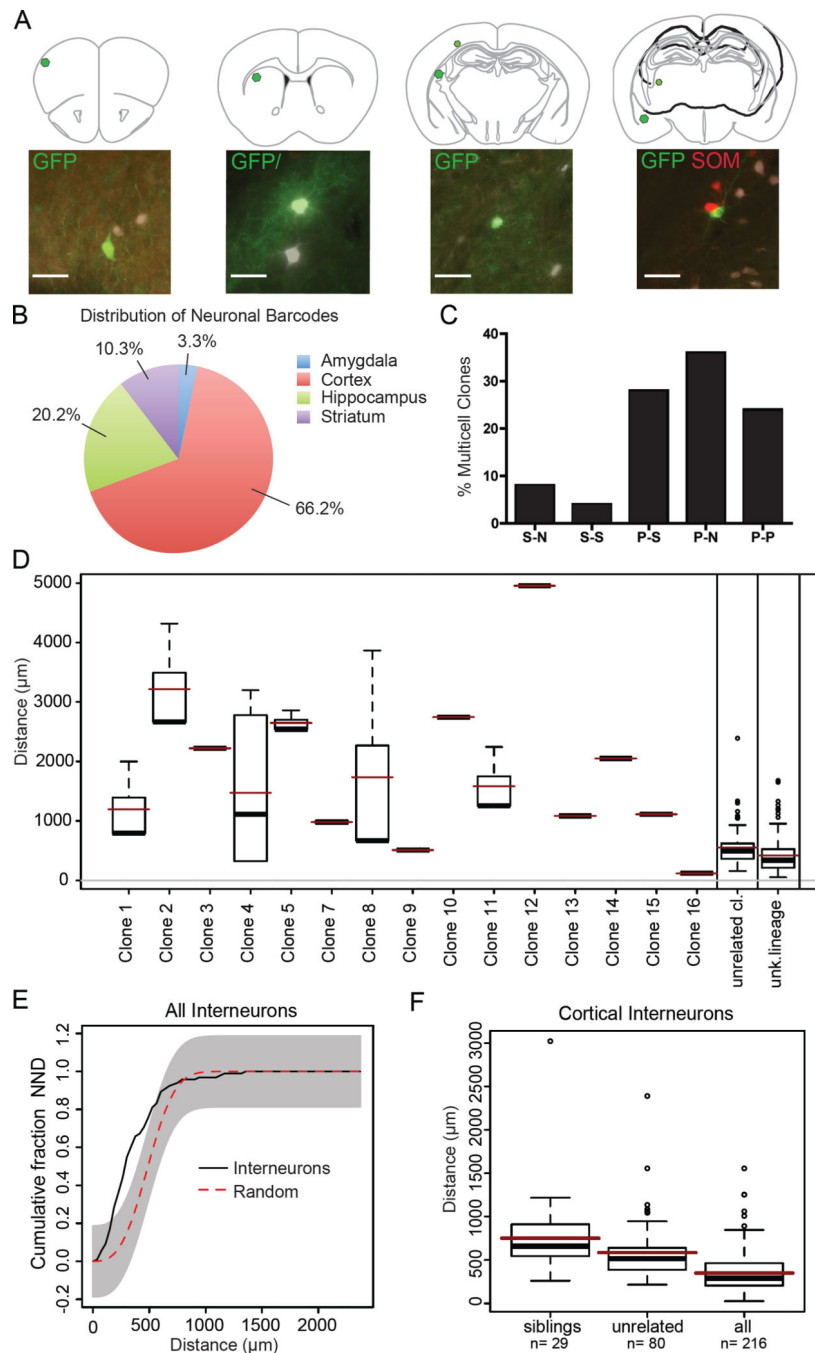


Figure 4. Interneuron Clones Consist of Widely Dispersed Cells of Diverse Subtypes

(A) Representative schematic of a four-cell clone containing three parvalbumin (PV) cells (white) and one somatostatin (SOM) cell (red) dispersed across thousands of microns in the brain. (B) Pie chart of forebrain regions which contain neurons that returned a barcode in Nkx2.1-Cre;LSL-Tva virus injected mice ($n = 302$ cells). (C) Bar graph showing the proportion of multi-cell clones composed of at least one cell type. S = somatostatin, P= parvalbumin, and N= negative for both markers ($n=84$ cells, 26 clones). (D) Box plot representing all of the nearest neighbor distances (NND) between pairs of cells in each

clone. The marks in the boxes are the 1st, 2nd (median) and 3rd quartile of the distances, with the dots representing the outliers. Superimposed red lines represent the mean distances in each group, and black bars represent the median distances (n = 2 brain hemispheres, 284 cells). (E) Cumulative (NND) of Nkx2.1-Cre;LSL-Tva brains (n = 284), with the gray area outlining 100 simulations of randomly distributed cells (complete spatial randomness). (F) Box plot representing NND of cortex cortical neurons. Sibling clones are significantly more widely distributed than unrelated cortical clones, and all neurons (both with and without tags) (multivs. single p < 0.01; multi vs. all p < 0.001, Kruskal-Wallis test) Scale bar: 50µm

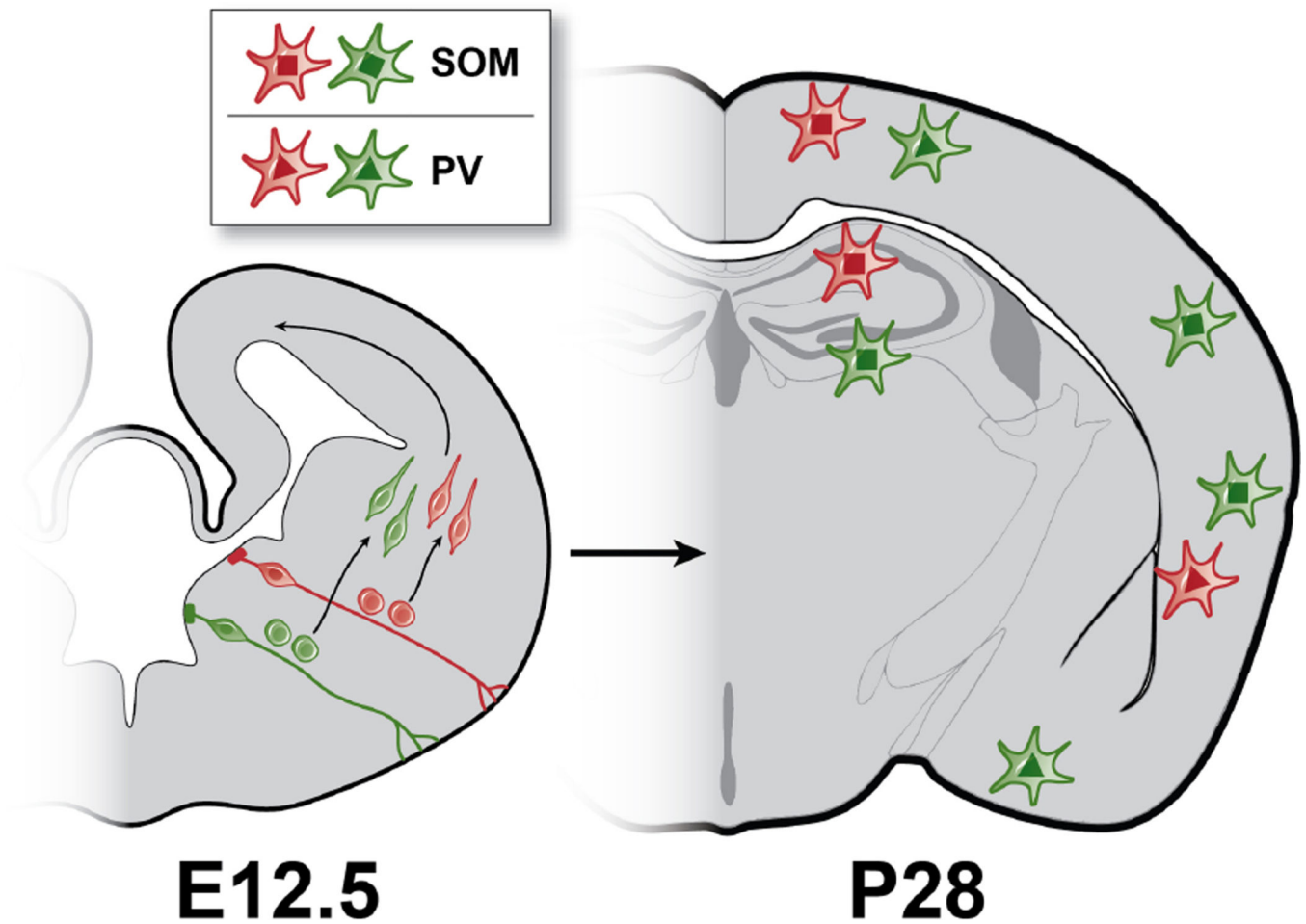


Figure 5. Wide Dispersion and Diversity of Clonally Related Interneurons

Left: Coronal section of embryonic (E12.5) mouse brain illustrating distinct clonal lineages of MGE progenitors (red and green). Radial glia must divide asymmetrically to produce intermediate progenitors cells, which divide symmetrically to produce pairs of newborn interneurons. The newborn neurons must then migrate tangentially to reach their final destinations in the forebrain. Right: Postnatal day (P28) mouse brain illustrating clones composed of SOM and PV subtypes dispersed widely across different functional and structural regions of the cortex, striatum (not shown) and hippocampus.